

Journal Pre-proof

Diabetes-associated sleep fragmentation impairs liver and heart function *via* SIRT1-dependent epigenetic modulation of NADPH oxidase 4

Yuanfang Guo, Jie Wang, Dongmei Zhang, Yufeng Tang, Quanli Cheng, Jiahao Li, Ting Gao, Xiaohui Zhang, Guangping Lu, Mingrui Liu, Xun Guan, Xinyu Tang, Junlian Gu

PII: S2211-3835(24)00488-X

DOI: <https://doi.org/10.1016/j.apsb.2024.12.031>

Reference: APSB 2212

To appear in: *Acta Pharmaceutica Sinica B*

Received Date: 18 July 2024

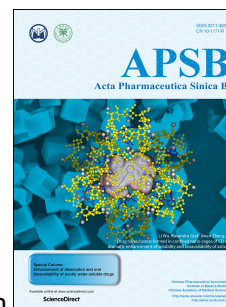
Revised Date: 29 October 2024

Accepted Date: 30 October 2024

Please cite this article as: Guo Y, Wang J, Zhang D, Tang Y, Cheng Q, Li J, Gao T, Zhang X, Lu G, Liu M, Guan X, Tang X, Gu J, Diabetes-associated sleep fragmentation impairs liver and heart function *via* SIRT1-dependent epigenetic modulation of NADPH oxidase 4, *Acta Pharmaceutica Sinica B*, <https://doi.org/10.1016/j.apsb.2024.12.031>.

This is a PDF file of an article that has undergone enhancements after acceptance, such as the addition of a cover page and metadata, and formatting for readability, but it is not yet the definitive version of record. This version will undergo additional copyediting, typesetting and review before it is published in its final form, but we are providing this version to give early visibility of the article. Please note that, during the production process, errors may be discovered which could affect the content, and all legal disclaimers that apply to the journal pertain.

© 2024 Published by Elsevier B.V. on behalf of Chinese Pharmaceutical Association and Institute of Materia Medica, Chinese Academy of Medical Sciences.



Original article

Diabetes-associated sleep fragmentation impairs liver and heart function *via* SIRT1-dependent epigenetic modulation of NADPH oxidase 4

Yuanfang Guo^{a,†}, Jie Wang^{a,†}, Dongmei Zhang^a, Yufeng Tang^b, Quanli Cheng^c, Jiahao Li^a, Ting Gao^a, Xiaohui Zhang^a, Guangping Lu^a, Mingrui Liu^a, Xun Guan^a, Xinyu Tang^a, Junlian Gu^{a,*}

^a*School of Nursing and Rehabilitation, Cheeloo College of Medicine, Shandong University, Jinan 250012, China*

^b*Department of Orthopedic Surgery, the First Affiliated Hospital of Shandong First Medical University, Jinan 250014, China*

^c*Department of Cardiovascular Disease, First Hospital of Jilin University, Changchun 130021, China*

Received 18 July 2024; received in revised form 29 October 2024; accepted 30 October 2024

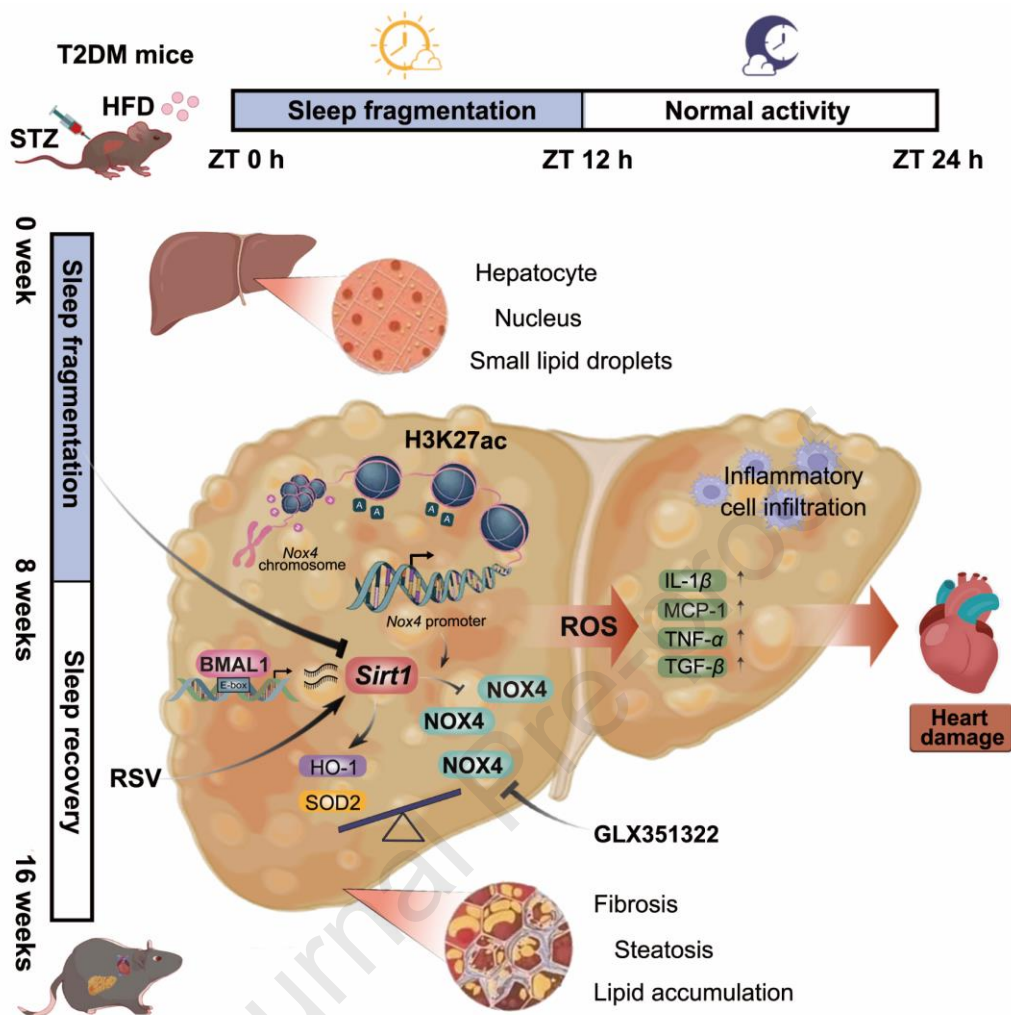
*Corresponding author.

E-mail address: junlian_gu@sdu.edu.cn (Junlian Gu).

†These authors made equal contributions to this work.

Running title: Role of MT1 in SF-aggravated testicular injury

Graphical abstract



The transcriptional regulation of SIRT1 by BMAL1 plays a pivotal role in linking the circadian clock to hepatic injury. Targeting the SIRT1–NOX4 axis presents a promising strategy for mitigating sleep fragmentation-induced cardio-hepatic damage.

Original article

Diabetes-associated sleep fragmentation impairs liver and heart function *via* SIRT1-dependent epigenetic modulation of NADPH oxidase 4

Yuanfang Guo^{a,†}, Jie Wang^{a,†}, Dongmei Zhang^a, Yufeng Tang^b, Quanli Cheng^c, Jiahao Li^a, Ting Gao^a, Xiaohui Zhang^a, Guangping Lu^a, Mingrui Liu^a, Xun Guan^a, Xinyu Tang^a, Junlian Gu^{a,*}

^a*School of Nursing and Rehabilitation, Cheeloo College of Medicine, Shandong University, Jinan 250012, China*

^b*Department of Orthopedic Surgery, the First Affiliated Hospital of Shandong First Medical University, Jinan 250014, China*

^c*Department of Cardiovascular Disease, First Hospital of Jilin University, Changchun 130021, China*

Received 18 July 2024; received in revised form 29 October 2024; accepted 30 October 2024

*Corresponding author.

E-mail address: junlian_gu@sdu.edu.cn (Junlian Gu).

†These authors made equal contributions to this work.

Running title: Detrimental SF memory in liver results in CVD

Abstract Although clinical evidence suggests that nonalcoholic fatty liver disease is an established major risk factor for heart failure, it remains unexplored whether sleep disorder-caused hepatic damage contributes to the development of cardiovascular disease (CVD). Here, our findings revealed that sleep fragmentation (SF) displayed notable hepatic detrimental phenotypes, including steatosis and oxidative damage, along with significant abnormalities in cardiac structure and function. All these pathological changes persisted even after sleep recovery for 2 consecutive weeks or more, displaying memory properties. Mechanistically, persistent higher expression of nicotinamide adenine dinucleotide phosphate oxidase 4 (NOX4) in the liver was the key initiator of SF-accelerated damage phenotypes. SF epigenetically controlled the acetylation of histone H3 lysine 27 (H3K27ac) enrichment at the *Nox4* promoter and markedly increased *Nox4* expression in liver even after sleep recovery. Moreover, fine coordination of the circadian clock and hepatic damage was strictly controlled by BMAL1-dependent Sirtuin 1 (*Sirt1*) transcription after circadian misalignment.

Accordingly, genetic manipulation of liver-specific *Nox4* or *Sirt1*, along with pharmacological intervention targeting NOX4 (GLX351322) or SIRT1 (Resveratrol), could effectively erase the epigenetic modification of *Nox4* by reducing the H3K27ac level and ameliorate the progression of liver pathology, thereby counteracting SF-evoked sustained CVD. Collectively, our findings may pave the way for strategies to mitigate myocardial injury from persistent hepatic detrimental memory in diabetic patients.

KEY WORDS Sleep fragmentation; Histone acetylation; Inter-organ communication; Non-alcoholic fatty liver disease; Heart disease; NOX4; SIRT1; Inflammation

1. Introduction

Although optimal sleep is integral to health and life, sleep disorders, such as obstructive sleep apnea, restless legs syndrome, and sleep fragmentation (SF), are highly prevalent and almost exclusively neglected among patients with type 2 diabetes mellitus (T2DM)¹. Particularly, SF in patients with T2DM becomes an increasingly important public health concern, which disrupts the function of several physiological systems including the impairment of critical metabolic and endocrine systems and the deregulation of redox and inflammatory processes. Although an adverse impact of SF on the risk of developing multiple pathological conditions, including obesity, insulin resistance, and diabetes, has been well established², we know little about the underlying cellular and molecular mechanisms that link SF to adverse cardiovascular outcomes in T2DM. Therefore, it is crucial to investigate the mechanisms by which SF contributes to cardiovascular damage and to develop more effective treatments for T2DM.

Frequent awakening of SF can disturb the circadian rhythm, ultimately leading to hypertension, dyslipidemia, and insulin resistance. Especially in the liver that contains a peripheral biological clock³, the circadian rhythm disruption can increase the risk of hepatic steatosis and systemic inflammation, emphasizing the key role of SF in the development of NAFLD⁴. If long-term circadian rhythm disorder cannot be efficiently repaired, it generally predisposes individuals to many comorbidities such as obesity and T2DM⁵. In mammals, inter-organ communication is essential for maintaining homeostasis under both physiological and pathological conditions. The interactions between the heart and liver are particularly intricate; cardiovascular diseases (CVD) can significantly affect liver homeostasis and *vice versa*^{6,7}. Notably, NAFLD is closely associated with adverse cardiac events, underscoring its potential as a pathogenesis-

independent risk factor for CVD^{8,9}. Nevertheless, it remains still largely unexplored whether SF-caused hepatic structural and functional abnormalities act as independent risk factors for major adverse cardiovascular events, including heart failure in T2DM.

Epigenetic modifications, an extensively studied mechanism for metabolic memory, exert an essential role in the pathogenesis and progression of many human diseases^{10,11}. Sleep homeostasis changes can either transiently or chronically affect chromatin modifications and epigenetic states, and unfavorable epigenetic changes are closely linked to an increased risk of obesity and T2DM¹². Notably, studies on metabolic memory in diabetes attributed to an increased risk of oxidative stress, immunological inflammation, and epigenetic modification. Among them, the initial activation of oxidative stress is specifically considered a critical early event in SF¹³. Accumulating evidence suggests that intracellular reactive oxygen species (ROS) can positively regulate the nuclear factor- κ B and NOD-, LRR- and pyrin domain-containing protein 3 inflammatory pathways, then promote the secretion of pro-inflammatory cytokines such as tumor necrosis factor- α (TNF- α), interleukin-1 β (IL-1 β), and monocyte chemoattractant protein-1 (MCP-1), ultimately exacerbating chronic inflammation phenotype and multiple organ failure¹⁴⁻¹⁶. As an abundant source of ROS production, the nicotinamide adenine dinucleotide phosphate (NADPH) oxidase (NOX) family could be tightly controlled by the stress-responsive signal transduction pathway¹⁷. Members of the NOX family, including NOX1, NOX2, and NOX4, are key sources of cellular hydrogen peroxide (H₂O₂) and ROS in the liver. Conversely, reductions in NOX activity are likely to promote redox balance and support metabolic homeostasis¹⁸⁻²⁰. However, it remains unclear whether and how NOX isoforms mediate SF-triggered hepatic oxidative damage and inflammatory responses in T2DM.

In this study, we aimed to investigate whether SF-mediated hepatic oxidative and inflammatory responses played a crucial role in cardiac pathogenesis and to further elucidate its potential mechanism. We characterized the promotive role of NOX4 in SF-triggered persistent hepatic oxidative and inflammatory phenotypes. SF epigenetically regulated the acetyl-histone H3K27 enrichment at the *Nox4* promoter and remarkably elevated *Nox4* expression in mouse liver tissue even after sleep recovery (SR). Moreover, the fine coordination of the circadian clock and hepatic damage was regulated by basic helix–loop–helix ARNT like 1 (BMAL1)-dependent Sirtuin 1 (*Sirt1*) transcription after SF challenge. Therefore, genetic manipulation of liver-specific *Nox4* or *Sirt1*, along with pharmacological intervention targeting NOX4 (GLX351322) or

SIRT1 (Resveratrol, RSV), could effectively mitigate the severity of hepatic injury phenotype, thereby counteracting SF-evoked sustained CVD. Collectively, our findings provide valuable insights into the pathophysiology of cardio-hepatic syndromes and predominantly highlight a previously unrecognized hepatic BMAL1–SIRT1–NOX4 axis as a promising therapeutic target for addressing SF-induced adverse health issues in the heart.

2. Materials and methods

2.1. Animals and treatments

Four sets of animal studies were conducted: (1) to assess the impact of SF and subsequent SR on cardiac and hepatic damage in mice with T2DM; (2) to investigate the role of hepatic NOX4 in SF-induced damage to the heart and liver; (3) to evaluate the epigenetic modification of SIRT1 on *Nox4* expression in the liver; and (4) to confirm the upstream circadian clock molecular regulators of SIRT1. All animal studies were conducted in accordance with the guidelines of the Ethics Committee of Shandong University (approval number: 2019-D-100). See Supporting Information (methods) for details.

2.2. Histopathology

Hematoxylin & eosin (H&E, Servicebio Technology, China) staining was performed to examine hepatic histological morphology. Lipid accumulation was detected by Oil red O staining according to the manufacturer's instructions (Sigma–Aldrich, MO, USA). Interstitial fibrosis was evaluated by Sirius red staining as previously described^{21,22}. The TNF- α levels, representing inflammatory response in the liver, were determined by immunohistochemical (IHC) staining. CD68 antibody (Proteintech, IL, USA), myeloperoxidase (MPO) antibody, and CD11b antibody (Servicebio, China) were used to stain macrophages and neutrophils. The images were taken using a Nikon E200 optical microscope and a Nikon TE2000-U inverted fluorescence microscope (Nikon, Tokyo, Japan). Image J was used to quantify the corresponding positive staining areas.

2.3. Dihydroethidium (DHE) and 2',7'-dichlorofluorescein diacetate (DCFH-DA) staining

Frozen liver tissue sections or cultured cells were fixed in cold methanol for 30 min and then incubated with 0.3% Triton X-100 for 30 min. After incubation, the tissue sections

or cultured cells were stained by 10 $\mu\text{mol/L}$ DHE or DCFH-DA (Sigma–Aldrich, MO, USA) for 30 min under dark conditions at 37 °C. The fluorescence images of each slide were observed by a fluorescence microscope (Nikon, Tokyo, Japan).

2.4. Recombinant adeno-associated virus serotype 8 (AAV8)

The adeno-associated virus serotype 8 (AAV8) delivery system was specifically used to knock down *Nox4* and overexpress *Sirt1* in the livers of mice. Recombinant AAV8 vectors carrying mouse *Nox4*-shRNA or *Sirt1*, along with the TBG (Serpin A7, a liver-specific expression protein) promoter (AAV8-TBG-CTL, AAV8-TBG-sh*Nox4*, AAV8-TBG-*Sirt1*), were provided by WZ Biosciences Inc. (China). Mice were injected with 200 μL virus containing 5×10^{11} AAV8 vector genome through a tail vein.

2.5. Chromatin immunoprecipitation (ChIP)

ChIP assays were performed using the Chromatin Immunoprecipitation Kit (Cell Signaling Technology, MA, USA). In brief, chromatin is partially digested with Micrococcal Nuclease to generate fragments, which are then subjected to overnight immunoprecipitation using antibodies specific for particular histone modifications (Abcam, Cambridge, UK). After protein–DNA decrosslinking, DNA is purified using a DNA purification centrifuge column (Cell Signaling Technology, MA, USA). qPCR is then employed to measure the amount of a specific DNA sequence that has been enriched through protein-specific immunoprecipitation.

2.6. Echocardiography

Cardiac function was determined by transthoracic echocardiography (Vevo 2100, Visual Sonics, Toronto, ON, Canada) in M mode on mice narcotized with isoflurane. Fractional shortening (FS), ejection fraction (EF), left ventricular internal dimension (LVID), interventricular septum thickness (IVS), and LV posterior wall thickness (LVPW) were measured and analyzed as our previously described^{21,22}.

2.7. Western blot analysis

Western blot assay was performed as our previously reported^{21,22}. The corresponding antibodies included: TNF- α (#ab307164, Abcam, Cambridge, UK), MCP-1 (#41987S, Cell Signaling Technology, MA, USA), SIRT1 (#8469S, Cell Signaling Technology, MA, USA), GAPDH (#2118S, Cell Signaling Technology, MA, USA), BMAL1

(#14020S, Cell Signaling Technology, MA, USA), CD68 (#28058-1-AP, Proteintech, IL, USA), NOX4 (#14347-1-AP, Proteintech, IL, USA), heme oxygenase-1 (HO-1) (#10701-1-AP, Proteintech, IL, USA), and superoxide dismutase 2 (SOD2) (#24127-1-AP, Proteintech, IL, USA). Expression levels were normalized to GAPDH.

2.8. Flow cytometry analysis

Samples of peripheral blood from mice were collected in anticoagulant tubes. Erythrocytes were lysed with RBC lysis buffer (Invitrogen, CA, USA). The remaining cells were washed with PBS and blocked with an Fc receptor-blocking solution (BioLegend, CA, USA). Subsequently, the cells were labeled with the following antibodies: CD45-eFlour 506, CD3-eFlour 450, CD4-allophycocyanin (APC)-eFlour 780, CD8-brilliant violet (BV) 650, B220-BV605, NK1.1-phycoerythrin (PE)-Cyanine 7, CD11b-PE (Invitrogen, CA, USA). The labeled cells were then analyzed using a flow cytometer (CytoFLEX S, Beckman Coulter, CA, USA).

2.9. Statistical analyses

All statistical analyses and graphs were performed using Graphpad Prism 9.5.0 software. All data were in line with normal distribution, and continuous variables were expressed as mean \pm standard deviation (SD). Student's *t*-test was used for the comparison of the means between 2 groups, and one-way analysis of variance or two-way analysis of variance was used for comparison between multiple groups of samples. Tukey's or Sidak's *post hoc* test was then conducted, and the statistical significance level was set at 0.05 ($P < 0.05$). Sample sizes, statistical methods, and *P* values are presented in the corresponding figure legends.

3. Results

3.1. SF exerts detrimental effects on liver and heart tissues, which displays a “memory” phenomenon after SR in T2DM mice

To investigate how SF might affect systemic injury, we first subjected T2DM mice to mechanical SF, tactilely rousing mice every 2 min during their rest period (Zeitgeber [ZT] 0–12 h) for 4 or 8 weeks (Supporting Information Fig. S1A). After the intervention process, no statistically discernable difference was identified in body weight gain between the CTL and SF groups (Fig. S1B), although it had been previously reported that SF directly caused obesity²³. However, 8 weeks of SF (SF8w) significantly

increased epididymal white adipose tissue (eWAT) mass in T2DM mice (Fig. S1C). To directly explore the effect of SF on glucose homeostasis and insulin sensitivity, glucose tolerance test (GTT) and insulin tolerance test (ITT), summarized areas under curves (AUCs), were performed as previously reported by our group²⁴. As expected, compared with the CTL8w group, SF8w group exhibited higher AUCs of GTT and ITT (Fig. 1A and B). Simultaneously, SF8w remarkably increased circulating levels of the lipid peroxidation marker malondialdehyde (MDA), while reducing the levels of the antioxidant glutathione (GSH) (Fig. 1C and D). Specifically, we measured the levels of circulating glutamic pyruvic transaminase (ALT) and glutamic oxaloacetic transaminase (AST) in serum. The results showed that the activities of ALT and AST were dramatically elevated after SF8w, which exhibited a severe liver injury phenotype in diabetic SF mice (Fig. 1E). Unexpectedly, in another batch of mice we purchased, although the ratio of AST/ALT underwent a dramatic change, there was no obvious difference in the ALT levels following SF treatment or other interventions. This inconsistency may be attributed to variations in factors such as the age, origin, and body weight of the mice. Furthermore, neither the systemic oxidative damage nor glucose tolerance and insulin sensitivity recovered to normal levels after SR (Fig. 1A–D). Similarly, the hepatic dysfunction induced by SF still persisted after SR (Fig. 1E), indicating the presence of a sustained state of liver injury.

Next, we further investigated the impact of SF on the pathogenesis of liver damage. Notably, SF significantly exacerbated abnormal morphology, lipid and collagen accumulation, and inflammation, as evidenced by H&E, Oil red O, Sirius red, and TNF- α IHC staining, respectively (Fig. 1F–I). These were supported by RT-qPCR and Western blot findings, which showed overtly upregulated fibrosis- and inflammation-related genes (*Il1b*, *Mcp1*, *Tnfa*, and transforming growth factor β (*Tgfb*)) and proteins (CD68, MCP-1, and TNF- α) (Fig. 1J–M and O–R). Furthermore, SF-treated mice also displayed a higher neutrophil infiltration (MPO) and macrophage infiltration (CD68 and CD11b) as observed by immunofluorescence staining (Fig. 1N). Collectively, these results demonstrated that SF significantly promoted a substantial increase in lipid accumulation, inflammation, and fibrosis in the livers of T2DM mice. Nevertheless, these adverse effects still persisted even after 2 weeks of SR (SR2w) (Fig. 1F–R), indicating that liver damage induced by SF exhibited a “memory” characteristic. Importantly, these persistent detrimental effects of SF showed little improvement, and

even more severe inflammatory phenotypes were observed after extending the period of normal sleep to 8 weeks (SR8w) (Fig. 2A–C).

Insert Fig. 1

The disruption of the circadian rhythm mechanism caused by SF can easily lead to NAFLD, which is a potentially independent risk factor for CVD^{8,9}. Accordingly, cardiac function was monitored by echocardiographic evaluation of left ventricular function, which was remarkably impaired after SF intervention, as evidenced by decreased EF and FS (Fig. 2D and E, Supporting Information Tables S2 and S3). SF diabetic mice also exhibited significantly exacerbated myocardial fibrosis, as illustrated by Masson staining of hearts (Fig. 2F and G). Similarly, SR failed to prevent the development of cardiac pathological and functional abnormalities (Fig. 2D–G). To find out how SF affected the cardiac function *in vivo*, the expression of inflammation- and fibrosis-related genes (*Il1b*, *Mcp1*, *Tnfa*, and *Tgfb*) in the hearts of T2DM mice was examined, and no significant difference was demonstrated between the SF and CTL groups (Fig. S1D). However, infiltrating inflammatory cells were clearly observed in the heart tissues of SF-treated T2DM mice (Fig. 2H), which suggests that the origin of inflammatory cells in the heart was not endogenous. As expected, serum levels of IL-1 β , MCP-1, TNF- α , and C-reactive protein (CRP) were elevated by SF, and consistently remained at high levels after SR (Fig. S1E). Moreover, we investigated the impact of SF on immune cells in peripheral blood by flow cytometry. After SF8w or SF8w-SR2w, the proportion of CD3⁺ T lymphocytes among CD45⁺ cells was observably decreased in peripheral blood compared to the CTL8w group (Fig. 2I and J). The proportion of CD4⁺ T cells among CD3⁺ T cells was significantly decreased, along with the CD4⁺/CD8⁺ ratio, while the proportion of CD8⁺ T cells among CD3⁺ T cells was increased compared to the CTL8w group (Fig. 2I and J, Fig. S1G). We also examined the abundance of B cells, NK cells, and CD11b⁺ myeloid cells in peripheral blood. No significant difference was observed in the proportion of B cells and NK cells among CD45⁺ cells between the SF8w and CTL8w groups (Fig. S1F and S1G). However, the proportion of CD11b⁺ myeloid cells among CD45⁺ cells was significantly increased in the SF8w and SF8w-SR2w groups (Fig. 2I and J). To further systemically evaluate the influence of SF on the pathogenesis of the heart, RNA sequencing (RNA-seq) was performed to characterize transcriptome-wide changes with or without SF in the hearts of T2DM mice. Cluster analysis showed that the two groups were clearly separated (Fig. S1H), suggesting an obvious difference between the CTL8w and SF8w groups. SF8w

could not achieve significant differences in cardiac chemokine-related genes (*e.g.*, C–C motif chemokine ligand 17 (*Ccl17*), C–X–C motif chemokine receptor 1 (*Cxcr1*) and C–X–C motif chemokine ligand 11 (*Cxcl11*)) and endogenous cytokine-related genes (*e.g.*, *Tnfa*, *Il6* and *Il1b*) in heart tissues as displayed by Volcano plot and Heatmap (Fig. 2K and L). Similarly, the SF8w group exhibited only a slight change but did not significantly impact oxidative stress- and circadian rhythm-related genes when compared to the CTL8w group, as displayed by Heatmap and Gene Set Enrichment Analysis (GSEA) (Fig. 2M–P).

Insert Fig. 2

3.2. Persistent high NOX4 expression contributes to adverse memory and massive liver damage in SF-treated T2DM mice

Substantial evidence has indicated that SF is closely associated with oxidative stress, which has been increasingly recognized as a contributing factor in inflammation-related diseases^{13,25}. Hence, we examined the effects of SF on the elicitation of oxidative stress in T2DM mice. SF could significantly induce hepatic ROS production, accompanied by increased MDA levels and decreased GSH levels, and these changes persisted after SR (Fig. 3A–C). Because NOX enzymes are major generators of ROS, which regulate the progression of hepatic pathological disorders, accordingly, we detected whether SF caused the upregulation of hepatic oxidative stress-related key factors (*Nox1*, *Nox2*, and *Nox4*). Our findings found hepatic *Nox4* mRNA change was earliest and most potent after SF challenge (Fig. 3D). Western blot further verified that NOX4 protein expression was upregulated by SF in liver tissues (Fig. 3E and F). To elucidate the transcriptional profile of the NOX family during acute-on-chronic liver failure, we performed bioinformatics processing and statistical analysis of RNA-seq data. Our analysis revealed that the upregulation of *Nox4*, rather than *Nox1* or *Nox2*, played a pivotal role in patients with alcoholic hepatitis (AH), hepatocellular carcinoma (HCC), acute liver failure (ALF), and hepatotoxicity (HT) (Fig. 3G and Supporting Information Fig. S2A). Likewise, there was a positive correlation between hepatic *Nox4* expression and liver dysfunction, as assessed by AST levels (Fig. 3H). Concomitantly, the expression levels of the classical antioxidant enzymes, such as HO-1 and SOD2, in the liver were significantly prohibited by SF8w and SF8w-SR2w (Fig. 3D–F). To our surprise, extending the SR time to 4 and 8 weeks did not alleviate hepatic oxidative stress damage, as evidenced by RT-qPCR and DHE staining in T2DM mice (Fig. S2B–

S2D).

To further verify the above *in vivo* results, the primary mouse hepatocytes were treated with H₂O₂, which was regarded as a more recognized cell model to mimic SF status *in vivo* as previously reported^{26,27}. Fig. 3I illustrated that the emergence of abnormal ROS formation might contribute to the subsequent inflammatory response observed in H₂O₂-stimulated primary mouse hepatocytes under high glucose (HG) conditions. Consistently, in HepG2 cells, treatment of H₂O₂ significantly increased cellular ROS levels with NOX4 elevation and subsequent activation of proinflammatory factors, which persisted after removal of H₂O₂ stimulus for 12 and 24 h, respectively (Fig. 3J–N). Taken together, NOX4-mediated oxidative stress may play a crucial role in the pathological processes underlying hepatic injury and the associated inflammatory response.

Insert Fig. 3

3.3. SF promotes NOX4 expression at the epigenetic level

Given that increased acetylation levels per histone are closely linked to active gene transcription, we proceeded to investigate the status of histone epigenetic modifications associated with the *Nox4* gene to elucidate the underlying mechanisms contributing to persistent hepatic damage following SR. Therefore, we screened 18 potential and most prominent types of histone modifications at the *Nox4* promoter region by using the Cistrome DB Toolkit (<http://dbtoolkit.cistrome.org>) (Fig. 4A). After focusing on liver tissue, we identified four potential types of histone modifications at the promoter region of *Nox4* (Fig. 4B). Next, the binding efficacy of H3K27ac, H3K4me1, H3K4me2, and H3K4me3 to the *Nox4* promoter region was detected by ChIP-qPCR, and the results demonstrated that enrichment of H3K27ac at the *Nox4* promoter region remarkably increased after SF8w. Importantly, this change of H3K27ac modification at the *Nox4* promoter region persisted even after SR2w. Other modifications of histone H3, such as H3K4me1, H3K4me2, and H3K4me3, did not exhibit significant differences between the SF8w and SF8w-SR2w groups in the liver tissues of T2DM mice when compared to the CTL8w group (Fig. 4C).

To further investigate the significance of *Nox4* epigenetic modification and its persistent upregulation in mouse liver tissue, we constructed mice with liver-specific *Nox4* knockdown using AAV8-TBG-sh*Nox4* (Fig. S2E). As expected, *Nox4* knockdown significantly alleviated SF-induced hepatic abnormal morphology, lipid

accumulation, fibrosis, and ROS production (Fig. 4D and E). This was accompanied by significant improvements in liver and serum levels of GSH and MDA, as well as ALT and AST activities (Fig. 4F–H) in T2DM mice. Simultaneously, the expression of proinflammatory cytokines and observed inflammatory cell infiltration, accompanied by an imbalance of cellular redox status, were recovered after *Nox4* knockdown in SF-treated T2DM mice (Fig. 4I–L). Furthermore, *Nox4* knockdown also effectively abolished SF-induced cardiac dysfunction and myocardial fibrosis (Fig. 4M and N, Supporting Information Table S4). Importantly, *Nox4* knockdown reversed the levels of inflammatory factors in the serum and effectively modulated the immune function in SF-treated T2DM mice (Fig. 4O and P, Supporting Information Fig. S4A–S4C). Consistent with these results, GLX351322, a specific NOX4 inhibitor, could also markedly mitigate SF-induced liver and heart injury phenotypes (Supporting Information Fig. S3 and Supporting Information Table S5). Consistently, we inhibited NOX4 expression in primary mouse hepatocytes exposed to H₂O₂ for 24 h, and the results were consistent with our *in vivo* studies (Fig. S4D–S4G). Moreover, as NOX4 is closely associated with ROS generation, to test whether ROS mediated hepatic inflammation, *N*-Acetyl-L-cysteine (NAC), a potent free-radical scavenger, was applied as a positive control to eliminate cellular ROS generation. Both NAC and GLX351322 effectively reversed H₂O₂-induced inflammation response in primary mouse hepatocytes under HG conditions (Fig. S4F and S4G). These observations collectively indicated that NOX4 inhibition exerts a protective antioxidant and anti-inflammatory function in the persistent cardio-hepatic injury caused by SF *in vivo* and cultured primary mouse hepatocytes *in vitro*.

Insert Fig. 4

3.4. *SIRT1* regulates the epigenetic modification of *Nox4*, thereby influencing hepatic oxidative stress and inflammatory responses

Generally, histone deacetylases (HDACs) exert a critical role as transcriptional modulators for gene expression. To comprehensively elucidate the potential function and discern the necessity of HDACs for NOX4 expression and hepatic injury, seven HDACs were targeted as they were previously testified to modulate NOX4 expression (Fig. 5A). Thus, the transcript levels of *Sirt1*, *Sirt2*, *Sirt3*, *Sirt6*, *Sirt7*, *Hdac1*, and *Hdac2* were assessed in our model. As observed in Fig. 5B, only the transcript level of *Sirt1* persistently declined after SF exposure in diabetic mouse liver tissue. SIRT1

expression at the protein level was further detected by Western blot analysis, and the results showed a significantly downregulated level of SIRT1 in the SF4w and SF4w-SR2w groups, which was continuously reduced in the SF8w and SF8w-SR2w groups (Fig. 5C). Subsequently, we further investigated whether SIRT1 was able to modulate epigenetic modifications of *Nox4*. The ChIP-qPCR results showed that increasing SIRT1 levels by RSV or AAV8-TBG-*Sirt1* significantly decreased the H3K27ac enrichment at the *Nox4* promoter region (Fig. 5D).

To further elucidate the anti-oxidative and anti-inflammatory effects of SIRT1, both loss- and gain-of-function approaches were employed using *Sirt1*-shRNA for silencing and the pcDNA3.1-*Sirt1* plasmid for overexpression in H₂O₂-stimulated primary mouse hepatocytes under HG conditions. Knockdown of *Sirt1* after H₂O₂ treatment for 24 h resulted in dramatic intracellular ROS (Fig. 5E and F) and proinflammatory cytokines production (Fig. 5I and J). However, GLX351322 substantially ameliorated H₂O₂-induced inflammation and oxidative stress in primary mouse hepatocytes transfected with *Sirt1*-shRNA (Fig. 5E, F, I, and J). Conversely, up-regulation of SIRT1 almost completely reversed H₂O₂-induced persistent inflammation and oxidative stress. It was noteworthy that GLX351322 could not further enhance the protective effects of SIRT1 on persistent inflammation and oxidative damage (Fig. 5G–J). Collectively, these data indicated that hepatic SIRT1 serves as a critical upstream molecule for the epigenetic modification of *Nox4*, which may be fundamental to the persistent liver injury caused by SF.

Insert Fig. 5

3.5. Liver-specific overexpression of *Sirt1* reverses SF-induced persistent oxidative and inflammatory stress in T2DM mice

To elucidate the impact of SIRT1 activation on SF-induced persistent injury in T2DM mice, liver-specific overexpression of *Sirt1* was achieved by tail vein injection of AAV8-TBG-*Sirt1* prior to T2DM mice with SF8w-SR2w (Supporting Information Fig. S5A). As expected, liver-specific overexpression of *Sirt1* markedly reduced lipid deposition and fibrosis, and also mitigated intracellular ROS accumulation compared to the control virus injection (AAV8-TBG-CTL) (Fig. 6A and B). Consistently, MDA levels in both liver and serum were dramatically reduced, alongside a marked decrease in ALT and AST activities, and GSH levels were notably increased after overexpression of *Sirt1* in the liver (Fig. 6C–E). Furthermore, liver-specific overexpression of *Sirt1* led

to an increase in hepatic antioxidant levels and effectively alleviated the persistent hepatic inflammatory response induced by SF. This was evidenced by significant upregulation in the protein and mRNA levels of HO-1 and SOD2, alongside a corresponding decrease in the levels of NOX4, CD68, MPO, CD11b, MCP-1, and TNF- α (Fig. 6F–H and Fig. S5B). Similar to these findings, RSV, an important pharmacological activator of SIRT1, exhibited consistent anti-inflammatory and antioxidant hepatoprotective effects in SF-treated T2DM mice (Fig. 6A–H and Fig. S5B). Notably, cardiac dysfunction and myocardial fibrosis were remarkably improved after liver-specific *Sirt1* overexpression or RSV treatment in SF-treated T2DM mice (Fig. 6I and J, Supporting Information Table S6). As expected, upregulation of SIRT1 inhibited the levels of inflammatory factors in the serum and effectively improved the immune function in SF-treated T2DM mice (Fig. 6K and L, Fig. S5C–S5E). In conclusion, these data illustrated that genetic or pharmacological activation of SIRT1 represents a promising therapeutic strategy to mitigate the destructive effects induced by SF in mice with T2DM.

Insert Fig. 6

3.6. *BMAL1* directly binds to *Sirt1* promoter and increases its transcription in T2DM mice with SF

Epidemiological studies revealed that circadian misalignment is strongly associated with the risk of a series of diseases, including NAFLD and T2DM⁴. SIRT1, a promising target for combating metabolic disorders in NAFLD²⁸, has been reported to exhibit circadian oscillations while being extensively regulated by the circadian clock²⁹. Accordingly, we further analyzed the potential upstream circadian clock molecular of SIRT1 in the present study. First, we subjected T2DM mice to SF intervention and detected the transcript levels of canonical core clock genes, including *Cry1*, *Cry2*, *Nr1d1* (also known as *REV-ERBa*), *Rora*, *Per1*, *Per2*, *Clock*, and *Bmal1*, at every eight-hour intervals for 24 h. Notably, our results displayed that the pattern of *Cry1*, *Cry2*, *Nr1d1*, *Rora*, and *Per1* gene expression did not show cyclical change of 24 h between groups with or without SF challenge (Fig. 7A–E). Interestingly, the expression of *Per2* and *Clock* was only modestly changed after the SF challenge around ZT16 and ZT8, respectively (Fig. 7F and G). However, the change of *Bmal1* was most prominent after the SF challenge at ZT0, ZT8, and ZT24 compared to the CTL group (Fig. 7H). Although knockdown of *Bmal1* and *Clock*, but not *Per2*, obviously decreased the

mRNA levels of *Sirt1* in HepG2 cells under circadian misalignment conditions (Fig. 7I and Supporting Information Fig. S6A–S6C), ChIP-qPCR analysis confirmed that BMAL1 directly bound to the *Sirt1* promoter and activated its expression, the effect of which was markedly disrupted by SF8w and SF8w-SR2w (Fig. 7J and K). Moreover, the downregulated SIRT1 expression at the mRNA and protein levels by knockdown of *Bmall* was subsequently validated in primary mouse hepatocytes under circadian misalignment conditions (Fig. 7L–N and Fig. S6D). Likewise, hepatocytes with *Bmall* silencing triggered higher fibrosis-related gene expression (*Tgfb* and *Ctgf*), intracellular ROS accumulation, and lipid overload (Fig. 7O–Q). Taken together, these findings demonstrated that BMAL1 binds to the *Sirt1* promoter region and activates signal transduction cascades, which can subsequently hinder the pathological processes in the liver after SF challenges.

Insert Fig. 7

4. Discussion

Emerging experimental and epidemiological evidence indicates that a high prevalence of sleep disorders is linked to the frequent occurrence of nighttime SF reported by patients with T2DM^{2,30}. SF is often associated with disruptions in glycolipid metabolism, insulin resistance, and the onset of diabetic complications^{2,31}. Despite its critical importance, the independent impact of SF on cardiovascular risk in T2DM remains largely undefined. The present work revealed that SF-mediated hepatic pathological and functional abnormalities contributed to the persistent adverse cardiac damage, in which the continuous high expression of NOX4-mediated oxidative stress exerted a key role in this process. Mechanically, we found the persistent high expression of *Nox4* caused by SF was a result of hyperacetylation modification of H3K27 at the *Nox4* promoter that was intricately controlled by SIRT1 deacetylase activity, the effect of which was almost completely improved and dampened by SIRT1 overexpression and knockdown, respectively.

The first important finding of this study was that hepatic oxidative damage and inflammation caused by SF displayed a “memory” feature and subsequently contributed to cardiac damage, which could not be rescued after SR. The liver performs a pivotal role in circadian rhythms and energy metabolism and displays multifaceted functional crosstalk with the heart⁶. Indeed, we observed that SF caused a marked increase in eWAT weight gain, dysregulated glucose homeostasis, and insulin resistance, and

importantly, sustained damage to the liver and heart function in T2DM mice. Meanwhile, SF-treated diabetic mice displayed higher lipid accumulation and fibrosis, accompanied by increased systemic inflammation and oxidative stress. Note that infiltration of neutrophils and macrophages was observed in cardiac tissues, but without a significant and discernable difference in inflammation-related gene expression, suggesting that the source of persistent inflammation in the heart was exogenous.

Activation of inflammatory processes, along with an imbalance in cellular redox status, is widely acknowledged as a predominant mechanism contributing to the pathogenesis of liver disease. Accordingly, we observed that SF elicited more positive fluorescent signals of ROS accumulation and decreased the expression of antioxidant factors (*e.g.*, GSH, HO-1, and SOD2) in liver tissues of T2DM mice. Given that the production of ROS, particularly superoxide, is primarily regulated by the NOX family, we proceeded to investigate which specific NOX subtypes are pivotal in this process. As previous studies reported, the levels of *Nox1/2/4* are primarily expressed in the liver³², and our results showed that only mRNA levels of *Nox2* and *Nox4* were significantly upregulated by SF. We thus focused mainly on the effect of NOX4 on the liver in the following study because of the relatively low expression level of NOX1 in the liver and high lethality of NOX2 deficient mice to T2DM^{33,34}. In the present study, we discovered a phenomenon of the earliest, most significant, and persistent upregulation of NOX4 expression, accompanied by functional and structural abnormalities in liver and heart tissues after SF in T2DM mice. Liver-specific *Nox4* knockdown and GLX351322, a highly specific inhibitor of NOX4, could remarkably abrogate SF-mediated oxidative stress and inflammatory injury in liver and heart tissues, implying that NOX4 plays a functional role in mediating diabetic cardio-hepatic injury in the face of SF challenge.

The second innovative finding of this study was that hyperacetylation modification of H3K27 played a key role in hepatic persistent high levels of NOX4 after SR. Several large population-based cohort studies have identified that the so-called “supplementary sleep” is not always sufficient to counteract the adverse effects of poor sleep quality³⁵⁻³⁷. One main reason for this phenomenon is that the brain undergoes adaptive changes during chronic sleep deprivation, which might exhibit too many detrimental effects on sleep structure or the neuroendocrine system. Besides, SF exposure has a more profound and lasting negative impact on the immune system of hematopoietic stem and progenitor cells through epigenetic modification. This persistent molecular imprinting

ultimately triggers inflammatory cascades, resulting in widespread inflammatory responses³⁷. In agreement, our results demonstrated that a two-week or longer span of SR was insufficient to prevent oxidative stress and inflammation in the liver triggered by SF. Similarly, T2DM mice exposed to SF exhibited both structural and functional abnormalities in the heart, with these deleterious effects persisting for 8 weeks or longer following SR. Thus, it is critical to elucidate the molecular and functional mechanisms underlying the prolonged effects of SF on adverse cardiac outcomes.

As is well established, epigenetic modification in the mammalian genome serves a causative role in regulating gene expression. For example, obstructive sleep apnea manipulates the epigenome of the cardiovascular system³⁸. Simultaneously, sleepless night alters the DNA methylation of transcription start sites of metabolic-related genes in adipose tissues of patients with T2DM³⁹. More importantly, changes in histone H3 acetylation induced by long-term SR are necessary to initiate a significant inflammatory response in the hematopoietic system³⁷. Based on our Western blotting and RT-qPCR results, which demonstrated that elevated NOX4 expression caused by SF still persisted after SR, we hypothesized that the sustained high levels of NOX4 might be governed by epigenetic programming. Indeed, subsequent experiments revealed a significant increase in the enrichment of H3K27ac at the *Nox4* promoter in the livers of diabetic SF/SR mice. This finding suggests that H3K27ac serves as a critical epigenetic regulatory mechanism underlying the persistent hepatic oxidative and inflammatory memory induced by chronic SF. Meanwhile, it is worth noting that regulation of NOX4 expression by transcription factor or post-transcription might be at play in our findings after chronic SF/SR exposure, which we need to further address in the following study.

Our third important finding was to clarify that SIRT1 was the main histone deacetylation modulator of NOX4, which maintained it in an inactive state. Following the database filtering, the major classes of histone deacetylases (*Hdac1*, *Hdac2*, *Sirt1*, *Sirt2*, *Sirt3*, *Sirt6*, and *Sirt7*) that predominantly reported to control NOX4 expression were evaluated in our model. The results showed that only SIRT1 expression continuously and significantly decreased in the presence of SF/SR challenge. It has been reported that SIRT1 is widely involved in many pathophysiological activities, such as inflammation, insulin secretion, extracellular matrix synthesis, and apoptosis, through regulating the activity of various signaling molecules by deacetylation⁴⁰⁻⁴³. Up-regulation of SIRT1 has beneficial effects on animal models of metabolic disorders, cognitive dysfunction, and cardiac dysfunction^{22,44-47}. To evaluate the potential role of

SIRT1 in regulating an aberrant histone modification of NOX4, we injected AAV8-TBG-*Sirt1* or RSV supplementation into mice to achieve liver-specific and systemic activation of SIRT1. CHIP-qPCR data indicated that the high expression of SIRT1 could dramatically reduce histone H3K27 acetylation at the promoter region of *Nox4*. Consistently, liver-specific overexpression of *Sirt1* improved liver damage by considerably mitigating hepatic lipid accumulation, inflammation, and oxidative stress, and therefore cardiac function was almost fully restored accordingly. Moreover, the application of specific SIRT1 activator RSV showed similar and powerful protective effects on the heart and liver, highlighting the promise for rapid translation into the clinic for interfering with the adverse effects of SF in patients with T2DM. Interestingly, we further revealed that BMAL1, as the upstream regulator of SIRT1, directly upregulated its transcription and contributed to its circadian change during the period of SF. Nevertheless, the underlying mechanisms by which SF-induced hepatic injury drives CVD might be complex. Further investigations are warranted to elucidate the precise role and underlying mechanisms of BMAL1 in SF-induced hepatic damage. Additionally, it is important to determine whether other members of the circadian clock gene family engage in similar epigenetic regulatory mechanisms that govern liver homeostasis within the context of the diabetic SF model. Furthermore, numerous studies have indicated that SF can disrupt the functioning of the hypothalamic-pituitary-adrenal (HPA) axis^{48,49}, and dysfunction of the HPA axis has been linked to T2DM, CVD, and metabolic dysfunction^{50,51}. Consequently, the intricate mechanisms through which SF influences liver and heart pathology by modulating the HPA axis in the context of the T2DM model require further investigation and clarification.

5. Conclusions

In conclusion, this study predominantly demonstrated that SF-induced oxidative and inflammatory damage in the livers of T2DM mice persisted even after the normalization of sleep patterns. This ongoing damage significantly influenced the communication between the liver and heart, ultimately contributing to cardiovascular impairment. The persistent high expression of NOX4 governed by SIRT1-mediated deacetylation of H3K27 played a key role in this process. We identified fine coordination of the circadian clock and hepatic damage by BMAL1-dependent *Sirt1* transcription after SF in diabetic liver. Genetic manipulation of liver-specific *Nox4* or *Sirt1*, along with pharmacological interventions targeting NOX4 (GLX351322) or SIRT1 (RSV), exerted robust protective

action against SF-induced hepatic oxidative and inflammatory phenotypes, highlighting the paramount importance of hepatic SIRT1/NOX4 pathway as a promising therapeutic target for CVD in T2DM patients with SF, as illustrated in Fig. 7R.

Acknowledgments

This work was supported by National Natural Science Foundation of China (No. 82272601), Young Taishan Scholars Program (No. TSQN202306013, China) and Natural Science Foundation of Shandong Province (No. ZR2021MH330, China). A special thanks goes to Prof. Jiyou Tang (Department of Neurology, Qianfoshan Hospital, Shandong First Medical University) for kindly providing the sleep deprivation apparatus. We also thank the Translational Medicine Core Facility of Shandong University for the consultation and instrument availability that supported this work.

Author contributions

Yuanfang Guo, Jie Wang and Yufeng Tang performed *in vivo* experiments and manuscript preparation; Dongmei Zhang, Quanli Cheng and Jiahao Li conducted *in vitro* experiments; Ting Gao and Xiaohui Zhang participated in data collection; Guangping Lu, Xun Guan, Xinyu Tang and Mingrui Liu contributed to data analysis. Yufeng Tang and Junlian Gu conceived the project and revised the manuscript; All of the authors approved the final version of the manuscript.

Conflicts of interest

The authors declare no conflict of interests.

References

- 1 Chattu VK, Chattu SK, Burman D, Spence DW, Pandi-Perumal SR. The interlinked rising epidemic of insufficient sleep and diabetes mellitus. *Healthcare-Basel* 2019; **7**: 37
- 2 Reutrakul S, Van Cauter E. Sleep influences on obesity, insulin resistance, and risk of type 2 diabetes. *Metabolism* 2018; **84**: 56-66
- 3 Guan D, Xiong Y, Trinh TM, Xiao Y, Hu W, Jiang C et al. The hepatocyte clock and feeding control chronophysiology of multiple liver cell types. *Science* 2020;

- 369:** 1388-94
- 4 Ferrell JM, Chiang JYL. Circadian rhythms in liver metabolism and disease. *Acta Pharm Sin B* 2015; **5**: 113-22
- 5 Eckel-Mahan KL, Patel VR, Mohny RP, Vignola KS, Baldi P, Sassone-Corsi P. Coordination of the transcriptome and metabolome by the circadian clock. *Proc Natl Acad Sci U S A* 2012; **109**: 5541-6
- 6 Cao Y, Wang Y, Zhou Z, Pan C, Jiang L, Zhou Z et al. Liver-heart cross-talk mediated by coagulation factor XI protects against heart failure. *Science* 2022; **377**: 1399-406
- 7 Xanthopoulos A, Starling RC, Kitai T, Triposkiadis F. Heart failure and liver disease cardiohepatic interactions. *Jacc-Heart Fail* 2019; **7**: 87-97
- 8 Targher G, Byrne CD, Tilg H. NAFLD and increased risk of cardiovascular disease: clinical associations, pathophysiological mechanisms and pharmacological implications. *Gut* 2020; **69**: 1691-705
- 9 Jin X, Qiu T, Li L, Yu R, Chen X, Li C et al. Pathophysiology of obesity and its associated diseases. *Acta Pharm Sin B* 2023; **13**: 2403-24
- 10 Kato M, Natarajan R. Epigenetics and epigenomics in diabetic kidney disease and metabolic memory. *Nat Rev Nephrol* 2019; **15**: 327-45
- 11 Shvedunova M, Akhtar A. Modulation of cellular processes by histone and non-histone protein acetylation. *Nat Rev Mol Cell Biol* 2022; **23**: 329-49
- 12 Ling C, Rönn T. Epigenetics in human obesity and type 2 diabetes. *Cell Metab* 2019; **29**: 1028-44
- 13 Zhang SX, Khalyfa A, Wang Y, Carreras A, Hakim F, Neel BA et al. Sleep fragmentation promotes NADPH oxidase 2-mediated adipose tissue inflammation leading to insulin resistance in mice. *Int J Obes (Lond)* 2014; **38**: 619-24
- 14 Yang N, Guo J, Wu H, Gao M, Xu S. Eucalyptol ameliorates chlorpyrifos-induced necroptosis in grass carp liver cells by down-regulating ROS/NF- κ B pathway. *Pestic Biochem Physiol* 2024; **198**: 105726
- 15 Lv T, Fan X, He C, Zhu S, Xiong X, Yan W et al. SLC7A11-ROS/ α KG-AMPK

- axis regulates liver inflammation through mitophagy and impairs liver fibrosis and NASH progression. *Redox Biol* 2024; **72**: 103159
- 16 Ribeiro MD, Szabo G. Role of the inflammasome in liver disease. *Annu Rev Pathol-Mech* 2022; **17**: 345-65
- 17 Schroder K. NADPH oxidases: current aspects and tools. *Redox Biol* 2020; **34**: 101512
- 18 Du J-J, Sun J-C, Li N, Li X-Q, Sun W-Y, Wei W. β -Arrestin2 deficiency attenuates oxidative stress in mouse hepatic fibrosis through modulation of NOX4. *Acta Pharmacol Sin* 2021; **42**: 1090-100
- 19 Zou Y, Chen Z, Sun C, Yang D, Zhou Z, Peng X et al. Exercise intervention mitigates pathological liver changes in NAFLD zebrafish by activating SIRT1/AMPK/NRF2 signaling. *Int J Mol Sci* 2021; **22**: 10940
- 20 Greatorex S, Kaur S, Xirouchaki CE, Goh PK, Wiede F, Genders AJ et al. Mitochondria- and NOX4-dependent antioxidant defense mitigates progression to nonalcoholic steatohepatitis in obesity. *J Clin Invest* 2024; **134**: e162533
- 21 Xiao M, Tang Y, Wang J, Lu G, Niu J, Wang J et al. A new FGF1 variant protects against adriamycin-induced cardiotoxicity via modulating p53 activity. *Redox Biol* 2022; **49**: 102219
- 22 Wang AJ, Tang Y, Zhang J, Wang BJ, Xiao M, Lu G et al. Cardiac SIRT1 ameliorates doxorubicin-induced cardiotoxicity by targeting sestrin 2. *Redox Biol* 2022; **52**: 102310
- 23 Muscogiuri G, Barrea L, Annunziata G, Di Somma C, Laudisio D, Colao A et al. Obesity and sleep disturbance: the chicken or the egg? *Crit Rev Food Sci Nutr* 2019; **59**: 2158-65
- 24 Gu JL, Yan XQ, Dai XZ, Wang YH, Lin Q, Xiao J et al. Metallothionein preserves Akt2 activity and cardiac function via inhibiting TRB3 in diabetic hearts. *Diabetes* 2018; **67**: 507-17
- 25 Gozal D, Khalyfa A, Qiao Z, Akbarpour M, Maccari R, Ottanà R. Protein-tyrosine phosphatase-1b mediates sleep fragmentation-induced insulin resistance and visceral adipose tissue inflammation in mice. *Sleep* 2017; **40**:

zsx111

- 26 Cubillos-Zapata C, Almendros I, Díaz-García E, Toledano V, Casitas R, Galera R et al. Differential effect of intermittent hypoxia and sleep fragmentation on PD-1/PD-L1 upregulation. *Sleep* 2020; **43**: zsz285
- 27 Li S, Tang L, Zhou J, Anchouche S, Li D, Yang Y et al. Sleep deprivation induces corneal epithelial progenitor cell over-expansion through disruption of redox homeostasis in the tear film. *Stem Cell Rep* 2022; **17**: 1105-19
- 28 da Silva Lima N, Fondevila MF, Nóvoa E, Buqué X, Mercado-Gómez M, Gallet S et al. Inhibition of ATG3 ameliorates liver steatosis by increasing mitochondrial function. *J Hepatol* 2022; **76**: 11-24
- 29 Zhou B, Zhang Y, Zhang F, Xia YL, Liu J, Huang R et al. CLOCK/BMAL1 regulates circadian change of mouse hepatic insulin sensitivity by SIRT1. *Hepatology* 2014; **59**: 2196-206
- 30 Schipper SBJ, Van Veen MM, Elders PJM, van Straten A, Van Der Werf YD, Knutson KL et al. Sleep disorders in people with type 2 diabetes and associated health outcomes: a review of the literature. *Diabetologia* 2021; **64**: 2367-77
- 31 Simonson M, Li Y, Zhu B, McAnany JJ, Chirakalwasan N, Sutabutr Vajaranant T et al. Multidimensional sleep health and diabetic retinopathy: Systematic review and meta-analysis. *Sleep Med Rev* 2024; **74**: 101891
- 32 Matuz-Mares D, Vázquez-Meza H, Vilchis-Landeros MM. NOX as a therapeutic target in liver disease. *Antioxidants (Basel)* 2022; **11**: 2038
- 33 Matsumoto M, Zhang J, Zhang X, Liu J, Jiang JX, Yamaguchi K et al. The NOX1 isoform of NADPH oxidase is involved in dysfunction of liver sinusoids in nonalcoholic fatty liver disease. *Free Radical Biology & Medicine* 2018; **115**: 412-20
- 34 Gray SP, Di Marco E, Okabe J, Szyndralewicz C, Heitz F, Montezano AC et al. NADPH oxidase 1 plays a key role in diabetes mellitus-accelerated atherosclerosis. *Circulation* 2013; **127**: 1888-902
- 35 Poroyko VA, Carreras A, Khalyfa A, Khalyfa AA, Leone V, Peris E et al. Chronic sleep disruption alters gut microbiota, induces systemic and adipose

- tissue inflammation and insulin resistance in mice. *Sci Rep* 2016; **6**: 35405
- 36 Depner CM, Melanson EL, Eckel RH, Snell-Bergeon JK, Perreault L, Bergman BC et al. Ad libitum weekend recovery sleep fails to prevent metabolic dysregulation during a repeating pattern of insufficient sleep and weekend recovery sleep. *Curr Biol* 2019; **29**: 957-67.e4
- 37 McAlpine CS, Kiss MG, Zuraikat FM, Cheek D, Schirotti G, Amatullah H et al. Sleep exerts lasting effects on hematopoietic stem cell function and diversity. *J Exp Med* 2022; **219**: e20220081
- 38 Chen YC, Hsu PY, Hsiao CC, Lin MC. Epigenetics: a potential mechanism involved in the pathogenesis of various adverse consequences of obstructive sleep apnea. *Int J Mol Sci* 2019; **20**: 2937
- 39 Cedernaes J, Schönke M, Westholm JO, Mi J, Chibalin A, Voisin S et al. Acute sleep loss results in tissue-specific alterations in genome-wide DNA methylation state and metabolic fuel utilization in humans. *Sci Adv* 2018; **4**: eaar8590
- 40 Zhu X, Su Q, Xie H, Song L, Yang F, Zhang D et al. SIRT1 deacetylates WEE1 and sensitizes cancer cells to WEE1 inhibition. *Nat Chem Biol* 2023; **19**: 585-95
- 41 Yang Y, Liu Y, Wang Y, Chao Y, Zhang J, Jia Y et al. Regulation of SIRT1 and its roles in inflammation. *Front Immunol* 2022; **13**: 831168
- 42 Lv X, Zhao Y, Yang X, Han H, Ge Y, Zhang M et al. Berberine potentiates insulin secretion and prevents β -cell dysfunction through the miR-204/SIRT1 signaling pathway. *Frontiers In Pharmacology* 2021; **12**: 720866
- 43 Lu H, Jia C, Wu D, Jin H, Lin Z, Pan J et al. Fibroblast growth factor 21 (FGF21) alleviates senescence, apoptosis, and extracellular matrix degradation in osteoarthritis via the SIRT1-mTOR signaling pathway. *Cell Death & Disease* 2021; **12**: 865
- 44 Yang Y, Wang X, Xiao A, Han J, Wang Z, Wen M. Ketogenic diet prevents chronic sleep deprivation-induced Alzheimer's disease by inhibiting iron dyshomeostasis and promoting repair via Sirt1/Nrf2 pathway. *Front Aging*

- Neurosci* 2022; **14**: 998292
- 45 Kang X, Jiang L, Lan F, Tang YY, Zhang P, Zou W et al. Hydrogen sulfide antagonizes sleep deprivation-induced depression- and anxiety-like behaviors by inhibiting neuroinflammation in a hippocampal Sirt1-dependent manner. *Brain Res Bull* 2021; **177**: 194-202
- 46 Song F, Lin J, Zhang H, Guo Y, Mao Y, Liu Z et al. Long-term sleep deprivation-induced myocardial remodeling and mitochondrial dysfunction in mice were attenuated by lipoic acid and N-Acetylcysteine. *Pharmaceuticals (Basel)* 2022; **16**: 51
- 47 Cui S, Hu H, Chen A, Cui M, Pan X, Zhang P et al. SIRT1 activation synergizes with FXR agonism in hepatoprotection via governing nucleocytoplasmic shuttling and degradation of FXR. *Acta Pharm Sin B* 2023; **13**: 559-76
- 48 van Dalftsen JH, Markus CR. The influence of sleep on human hypothalamic-pituitary-adrenal (HPA) axis reactivity: A systematic review. *Sleep Med Rev* 2018; **39**: 187-94
- 49 Tapp ZM, Cornelius S, Oberster A, Kumar JE, Atluri R, Witcher KG et al. Sleep fragmentation engages stress-responsive circuitry, enhances inflammation and compromises hippocampal function following traumatic brain injury. *Exp Neurol* 2022; **353**: 114058
- 50 Gan L, Li N, Heizati M, Lin M, Zhu Q, Hong J et al. Diurnal cortisol features with cardiovascular disease in hypertensive patients: a cohort study. *Eur J Endocrinol* 2022; **187**: 629-36
- 51 Janssen JAMJL. New insights into the role of insulin and hypothalamic-pituitary-adrenal (HPA) axis in the metabolic syndrome. *Int J Mol Sci* 2022; **23**: 8178

Figure captions

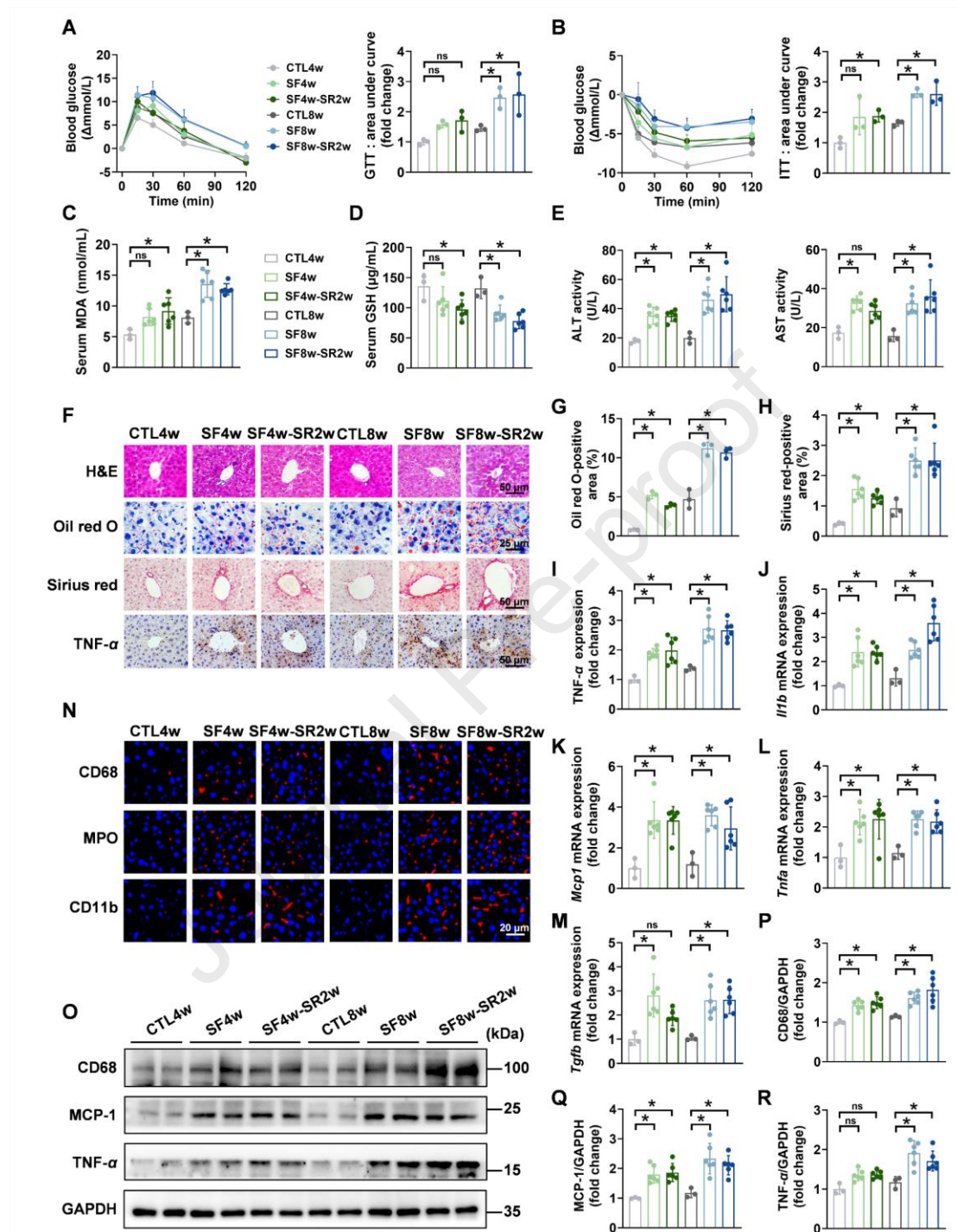
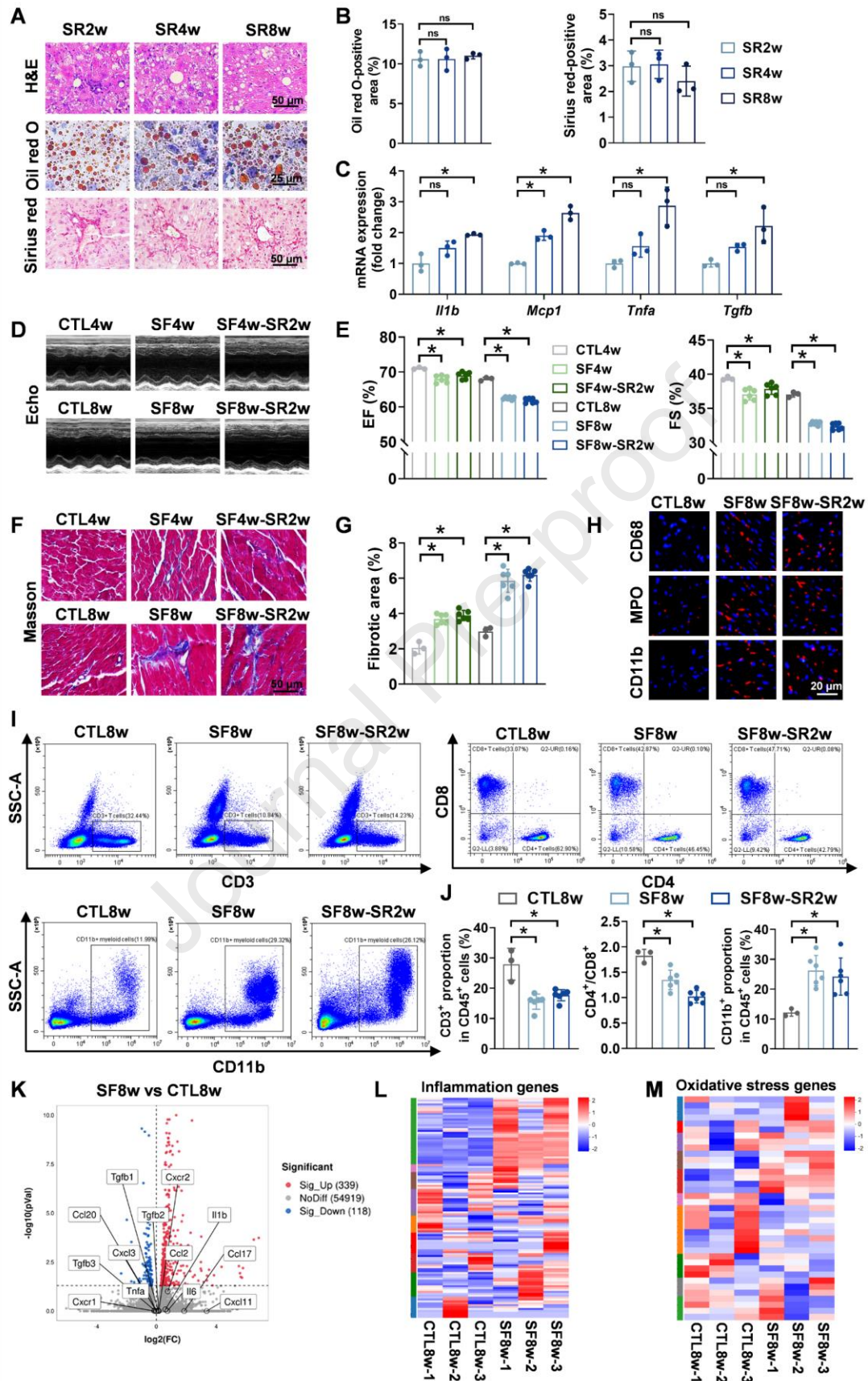


Figure 1 SF exerts a prolonged detrimental effect on liver in T2DM mice. (A, B) Blood glucose of T2DM mice with or without SF/SR at 0, 30, 60, 90, and 120 min after glucose/insulin injection was detected by GTT and ITT. (C, D) The levels of MDA and GSH in serum. (E) Serum ALT and AST activities were assayed. (F) Representative images of liver sections stained with H&E, Oil red O, Sirius red, and IHC staining of

TNF- α . (G–I) Quantitative analysis of adipose deposition area, fibrosis area, and TNF- α protein level in liver tissues. (J–M) Relative mRNA levels of *Illb*, *Mcp1*, *Tnfa*, and *Tgfb* in liver tissues were detected by RT-qPCR. (N) Representative immunofluorescence staining images of CD68, MPO, and CD11b (red) in liver sections. The nucleus was labeled with DAPI (blue). (O–R) The protein levels of CD68, MCP-1, and TNF- α in liver tissues were detected by Western blot. GAPDH was used for internal control. Data are expressed as mean \pm SD, $n = 3–6$. * $P < 0.05$. ns indicates no significance. CTL4w/8w: T2DM mice without SF; SF4w/8w: T2DM mice with 4 or 8 weeks of SF; SR2w: 2 weeks after SR in T2DM mice.



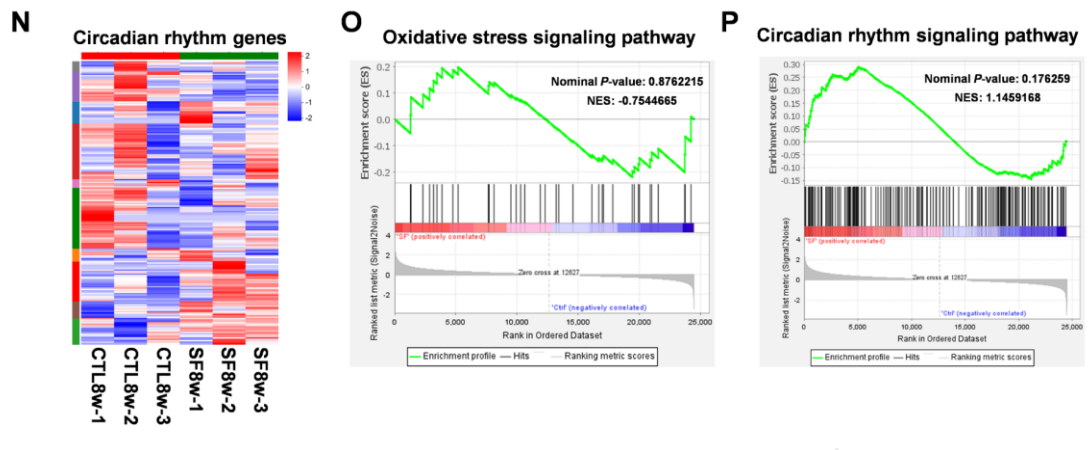


Figure 2 SF-induced hepatic and cardiac pathological abnormalities cannot be alleviated by SR in T2DM mice. (A, B) Representative images and quantitative analyses of H&E, Oil red O, and Sirius red staining in liver tissues of T2DM mice with SF8w after the extension of SR2w to SR8w. (C) Relative mRNA levels of *Il1b*, *Mcp1*, *Tnfa*, and *Tgfb* were detected by RT-qPCR in liver tissues of T2DM mice with SF8w after the extension of SR2w to SR8w. (D, E) Cardiac function was examined by echocardiography. (F, G) Representative images and quantitative analysis of Masson staining of heart sections. (H) Representative images of CD68, MPO, and CD11b (red) immunofluorescence staining of heart sections. The nucleus was labeled with DAPI (blue). (I) Flow cytometry plots showing CD3⁺ T cells, CD4⁺ T cells, CD8⁺ T cells, and CD11b⁺ myeloid cells in peripheral blood. (J) Statistical analysis of the proportions of CD3⁺ T cells and CD11b⁺ myeloid cells and CD4⁺/CD8⁺ ratio. (K) The Volcano plot of differential expression gene identified by RNA sequencing between the CTL8w and SF8w groups. (L–N) Heatmap of inflammation-, oxidative stress-, and circadian rhythm-related genes between the CTL8w and SF8w groups (O, P) GSEA enrichment analysis of oxidative stress- and circadian rhythm-related genes between the CTL8w and SF8w groups. Data are presented as mean \pm SD, $n = 3-6$. * $P < 0.05$. ns indicates no significance.

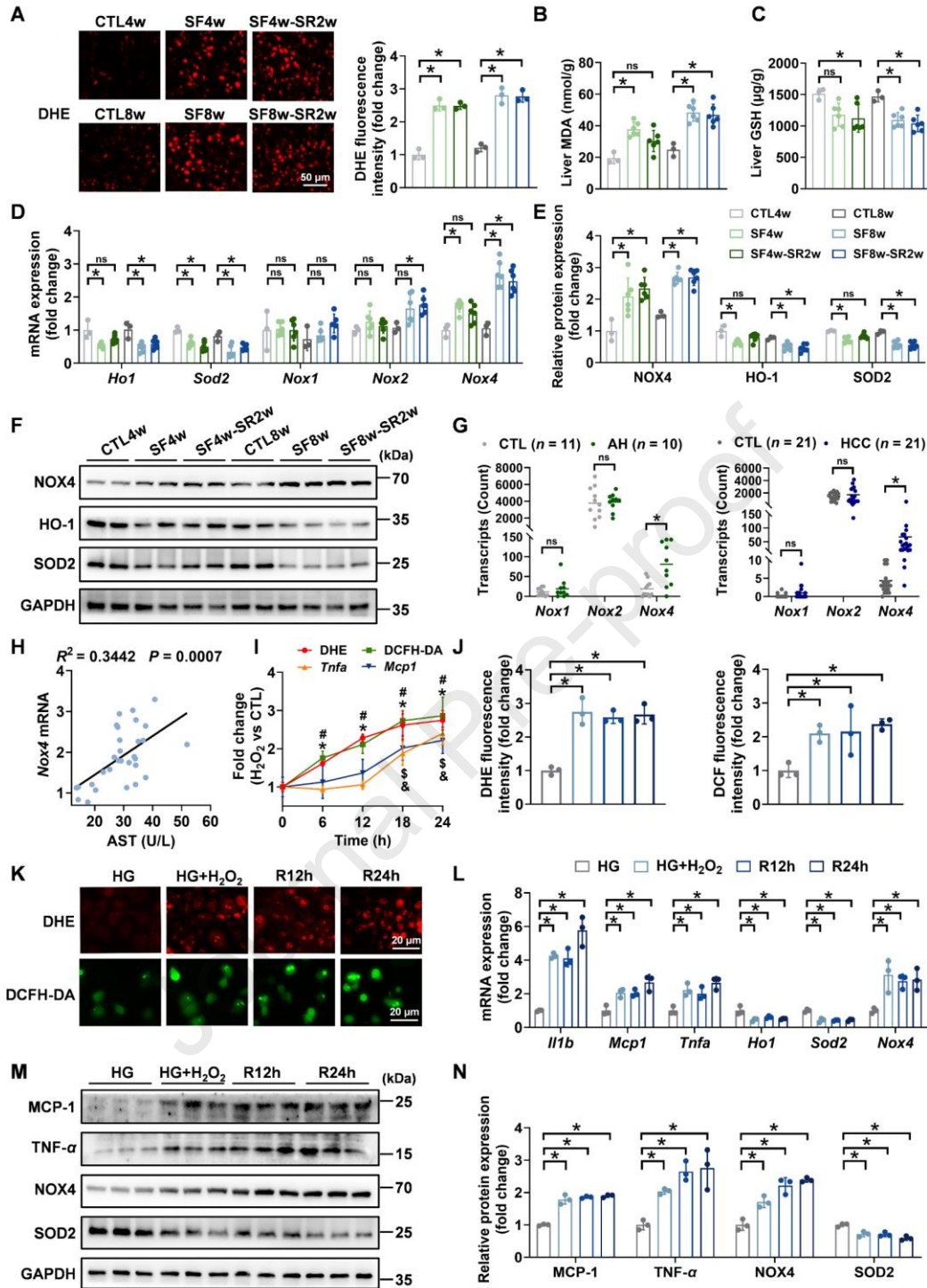


Figure 3 NOX4 contributes to hepatic adverse memory in SF-treated T2DM mice. (A) Representative images of DHE staining and quantitative analysis of fluorescence intensity in liver sections. (B, C) The levels of MDA and GSH in liver tissues. (D) Relative mRNA levels of *Ho1*, *Sod2*, *Nox1*, *Nox2*, and *Nox4* in liver tissues were detected by RT-qPCR. (E, F) The protein levels of NOX4, HO-1, and SOD2 in liver tissues were detected by Western blot. (G) *Nox1*, *Nox2*, and *Nox4* expression in

population databases of normal people and patients with alcoholic hepatitis (AH) and hepatocellular carcinoma (HCC). (H) Correlation analysis of AST and *Nox4* mRNA level. (I) The levels of *Tnfa* mRNA, *Mcp1* mRNA as well as DHE and DCF fluorescence intensity in HG-treated primary mouse hepatocytes after H₂O₂ treatment for 0, 6, 12, 18, and 24 h. **P* < 0.05 vs. 0 h represents DHE fluorescence intensity, #*P* < 0.05 vs. 0 h represents DCF fluorescence intensity, \$*P* < 0.05 vs. 0 h represents *Tnfa* mRNA levels, &*P* < 0.05 vs. 0 h represents *Mcp1* mRNA levels. (J, K) HepG2 cells were treated with H₂O₂ for 24 h under the HG condition, and then the H₂O₂ stimulus was removed for 12 and 24 h, respectively. Representative images and fluorescence intensity quantitative analyses of DHE and DCFH-DA staining of HepG2 cells. (L) Relative mRNA levels of *Il1b*, *Mcp1*, *Tnfa*, *Hol*, *Sod2*, and *Nox4* in HepG2 cells were detected by RT-qPCR. (M, N) The protein levels of MCP-1, TNF- α , NOX4, and SOD2 in HepG2 cells were detected by Western blot. GAPDH was used as an internal control. Data are presented as mean \pm SD, *n* = 3–6 for mouse test, *n* = 3 for cell test. **P* < 0.05. ns indicates no significance.

Figure 4 SF promotes NOX4 expression at the epigenetic level. (A) The most likely histone modifications at the *Nox4* promoter region in different tissues and cell lines were screened. (B) The 4 most likely histone modifications at the *Nox4* promoter region were targeted in the liver. (C) The relative binding levels of H3K27ac, H3K4me1, H3K4me2, and H3K4me3 on the *Nox4* promoter in liver tissues of T2DM mice with or without SF/SR were measured by ChIP-qPCR ($n = 3$). (D, E) Representative images and quantitative analyses of liver sections stained with H&E, Oil red O, Sirius red, and DHE staining. (F) The activities of ALT and AST in serum. (G, H) The levels of MDA and GSH in serum and liver tissues. (I, J) The protein levels of CD68, MCP-1, TNF- α , NOX4, HO-1, and SOD2 in liver tissues were detected by Western blot. (K) Representative images of CD68, MPO, and CD11b (red) immunofluorescence staining in liver tissues. The nucleus was labeled with DAPI (blue). (L) Relative mRNA levels of *Il1b*, *Mcp1*, *Tnfa*, *Tgfb*, *Ho1*, and *Sod2* were detected by RT-qPCR. (M, N) Cardiac function and myocardial fibrosis were determined by echocardiography and Masson staining. (O) Flow cytometry plots showing CD3⁺ T cells, CD4⁺ T cells, CD8⁺ T cells, and CD11b⁺ myeloid cells in peripheral blood. (P) Statistical analysis of the proportions of CD3⁺ T cells, CD4⁺ T cells, CD8⁺ T cells, and CD11b⁺ myeloid cells and CD4⁺/CD8⁺ ratio. GAPDH was used for internal control. Data are presented as mean \pm SD, $n = 6$. * $P < 0.05$. ns indicates no significance.

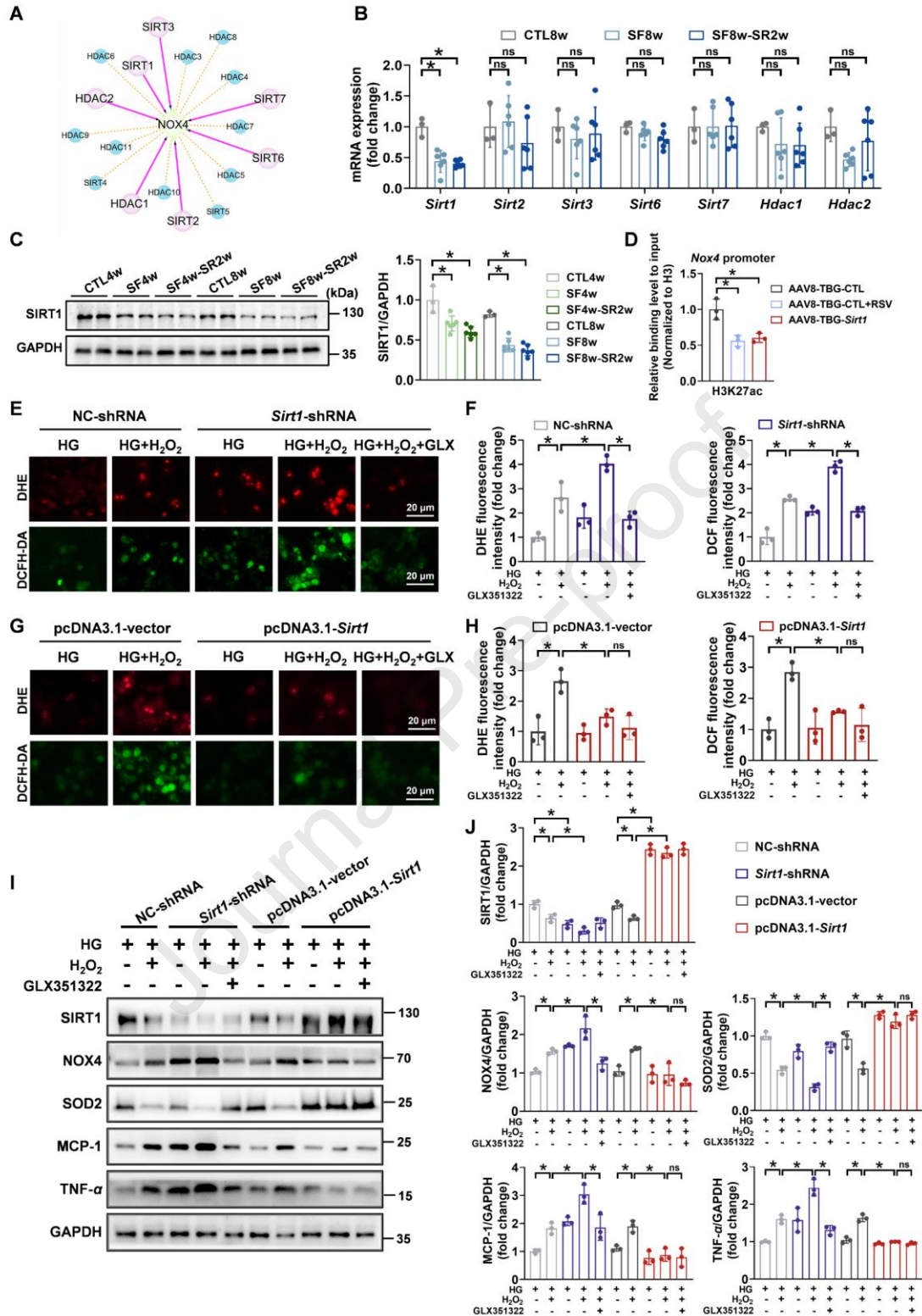


Figure 5 SIRT1 controls the epigenetic modification of *Nox4* and hepatic oxidative and inflammatory stress. (A) The histone deacetylases that regulate *Nox4* (solid line). (B) Relative mRNA levels of *Sirt1*, *Sirt2*, *Sirt3*, *Sirt6*, *Sirt7*, *Hdac1*, and *Hdac2* in liver tissues of T2DM mice with or without SF/SR were detected by RT-qPCR. (C) The

expression of SIRT1 in liver tissues of T2DM mice with or without SF/SR was analyzed by Western blot. (D) The relative binding levels of H3K27ac on the *Nox4* promoter in liver tissues. (E, F) Representative images and fluorescence intensity quantitative analyses of DHE (red) and DCFH-DA staining (green) after transfection of NC-shRNA or *Sirt1*-shRNA in primary mouse hepatocytes. (G, H) Representative images and fluorescence intensity quantitative analyses of DHE (red) and DCFH-DA staining (green) after transfection of pcDNA3.1-vector or pcDNA3.1-*Sirt1* in primary mouse hepatocytes. (I, J) Western blot analysis and density quantification of SIRT1, NOX4, SOD2, MCP-1, and TNF- α in primary mouse hepatocytes transfected with NC-shRNA, *Sirt1*-shRNA, pcDNA3.1-vector or pcDNA3.1-*Sirt1*. GAPDH was used for internal control. Data are presented as mean \pm SD, $n = 3-6$ for mouse test, $n = 3$ for cell test. * $P < 0.05$. ns indicates no significance.

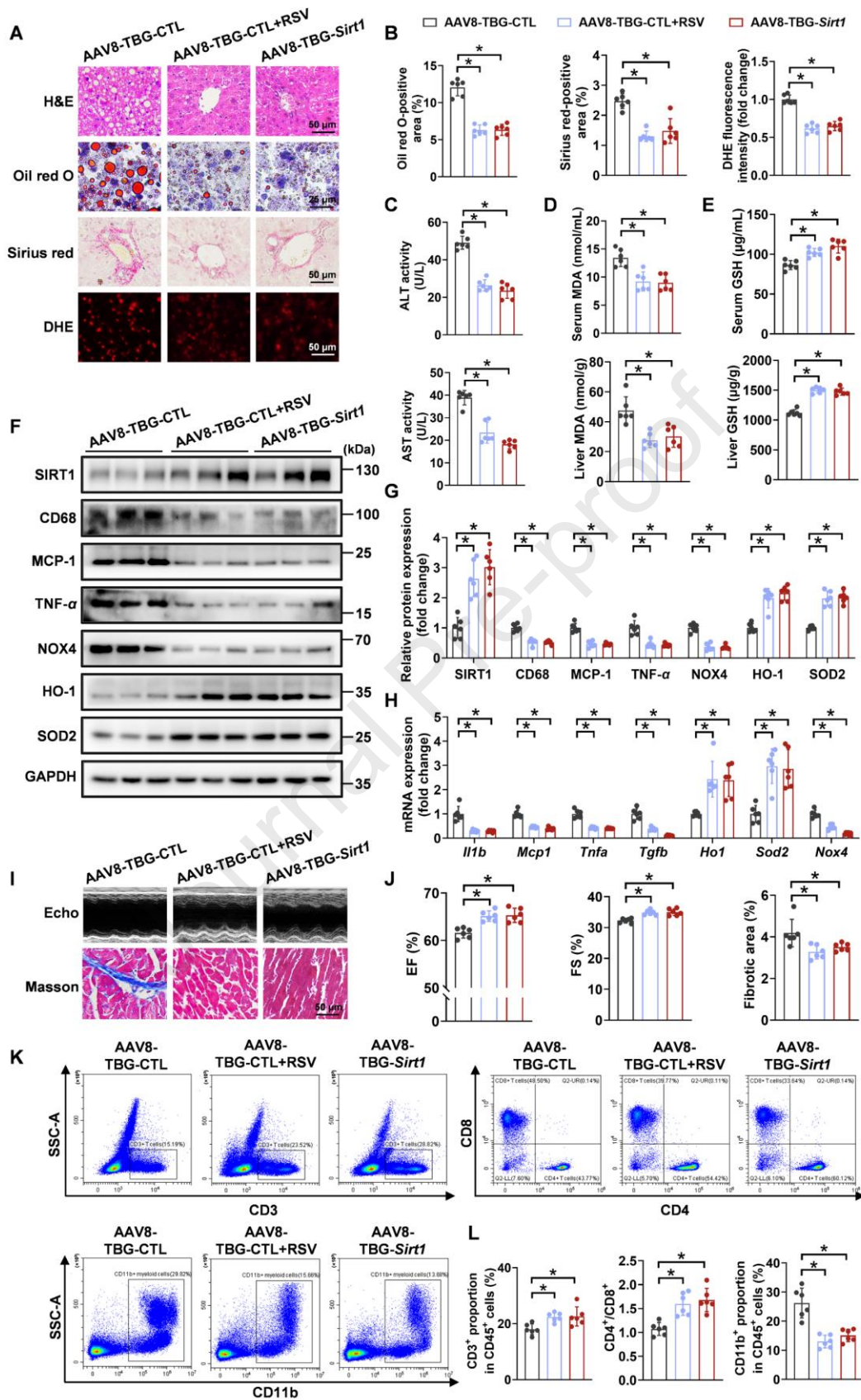


Figure 6 Liver-specific overexpression of *Sirt1* reverses SF-induced persistent oxidative and inflammatory stress. (A, B) Representative images and corresponding

quantitative analyses of H&E, Oil Red O, Sirius red, and DHE staining in liver sections. (C) The activities of ALT and AST in serum. (D, E) The levels of MDA and GSH in serum and liver tissues. (F, G) The protein levels of SIRT1, CD68, MCP-1, TNF- α , NOX4, HO-1, and SOD2 in liver tissues were detected by Western blot. (H) Relative mRNA levels of *Il1b*, *Mcp1*, *Tnfa*, *Tgfb*, *Ho1*, *Sod2*, and *Nox4* were detected by RT-qPCR. (I, J) Cardiac function and myocardial fibrosis were determined by echocardiography and Masson trichrome staining. (K) Flow cytometry plots showing CD3⁺ T cells, CD4⁺ T cells, CD8⁺ T cells, and CD11b⁺ myeloid cells in peripheral blood. (L) Statistical analysis of the proportions of CD3⁺ T cells and CD11b⁺ myeloid cells and CD4⁺/CD8⁺ ratio. GAPDH was used for internal control. Data are presented as mean \pm SD, $n = 6$. * $P < 0.05$. ns indicates no significance.

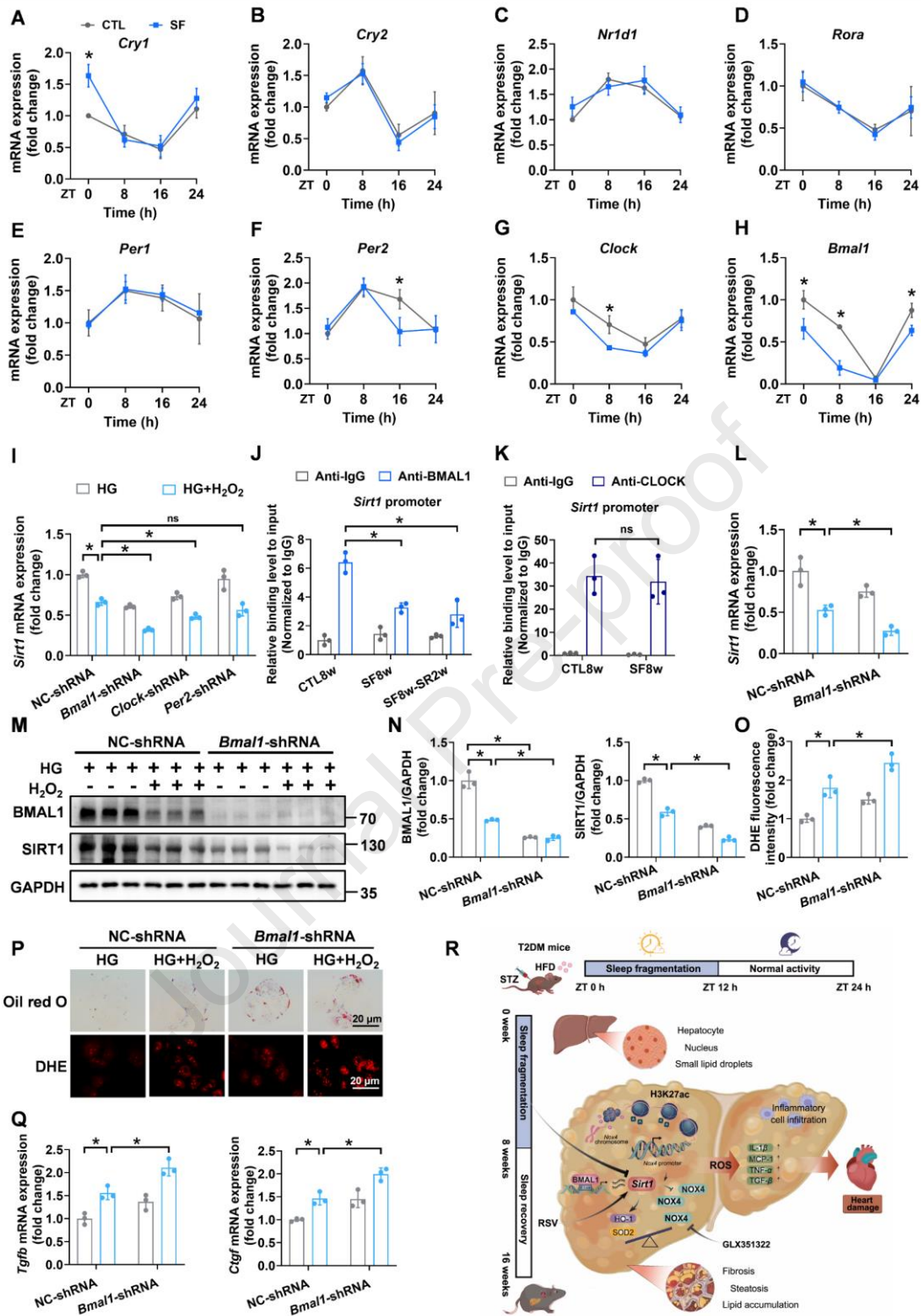


Figure 7 BMAL1 directly binds to the *Sirt1* promoter and increases its transcription in T2DM mice with SF. (A–H) Canonical core clock genes *Cry1*, *Cry2*, *Nr1d1*, *Rora*, *Per1*, *Per2*, *Clock*, and *Bmal1* at every eight-hour interval for 24 h were detected by RT-qPCR. (I) *Sirt1* mRNA level was examined by RT-qPCR after knockdown of *Bmal1*, *Clock*, and *Per2* in HepG2 cells. (J, K) BMAL1 and CLOCK bound to the *Sirt1* promoter

region as demonstrated by ChIP-qPCR assay. (L) *Sirt1* mRNA level was examined by RT-qPCR after the knockdown of *Bmal1* in primary mouse hepatocytes. (M, N) The protein levels of BMAL1 and SIRT1 were examined by Western blot after the knockdown of *Bmal1* in primary mouse hepatocytes. (O, P) Representative images and fluorescence intensity quantitative analysis of Oil red O and DHE staining after transfection of NC-shRNA or *Bmal1*-shRNA in HepG2 cells. (Q) Relative mRNA levels of fibrosis-related genes *Tgfb* and *Ctgf* were detected by RT-qPCR after transfection of NC-shRNA or *Bmal1*-shRNA in primary mouse hepatocytes. (R) A mechanistic illustration of SF-induced hepatic damage to drive CVD in T2DM mice. GAPDH was used for internal control. Data are presented as mean \pm SD, $n = 3$. $*P < 0.05$. ns indicates no significance.